

Why scaling up uncertain predictions to higher levels of organisation will underestimate change

James Orr*, Jeremy Piggott, Andrew Jackson, and Jean-François Arnoldi

*Zoology department, School of Natural Sciences,
Trinity College Dublin, The University of Dublin, Ireland.*

**jaorr@tcd.ie*

September 22, 2020

Abstract

1
2 Uncertainty is an irreducible part of predictive science, causing us to over- or underestimate
3 the magnitude of change that a system of interest will face. In a reductionist approach, we may
4 use predictions at the level of individual system components (e.g. species biomass), and combine
5 them to generate predictions for system-level properties (e.g. ecosystem function). Here we
6 show that this process of scaling up uncertain predictions to higher levels of organization has
7 a surprising consequence: it will systematically underestimate the magnitude of system-level
8 change, an effect whose significance grows with the system's dimensionality. This stems from a
9 geometrical observation: in high dimensions there are more ways to be more different, than ways
10 to be more similar. This general remark applies to any complex system. Here we will focus on
11 ecosystems thus, on ecosystem-level predictions generated from the combination of predictions
12 at the species-level. In this setting, the ecosystem's dimensionality is a measure of its diversity.
13 We explain why dimensional effects do not play out when predicting change of a single linear
14 aggregate property (e.g. total biomass), yet are revealed when predicting change of non-linear
15 properties (e.g. absolute biomass change, stability or diversity), and when several properties
16 are considered at once to describe the ecosystem, as in multi-functional ecology. Our findings
17 highlight and describe the counter-intuitive effects of scaling up uncertain predictions, effects that
18 will occur in any field of science where a reductionist approach is used to generate predictions.

19 **Keywords:** Ecological Complexity, Diversity Metrics, Dimensionality, Mechanistic prediction,
20 Multi-functionality, Multiple Stressors, Reductionism.

21 1 Introduction

22 In natural sciences, uncertainty of any given prediction is ubiquitous (Dovers & Handmer,
23 1992). When considering predictions of change, uncertainty has directional consequences:
24 uncertain predictions will lead to either over- or underestimation of actual change. The
25 reductionist approach to complex systems is to gather and use knowledge about individual
26 components before scaling up predictions to the system-level (Levins & Lewontin, 1985; Wu,
27 Jones, Li, & Loucks, 2006). Although scaling up to higher levels of organisation is general
28 to the study of any complex systems, it is particularly well-defined in ecology. In this field,
29 knowledge about the components at lower levels of organisation (individuals, populations)
30 is commonly used to understand the systems at higher levels of organisation (communities,
31 ecosystems) (Loreau, 2010; Woodward, Perkins, & Brown, 2010).

32 An unbiased prediction of an individual component is one that makes no systematic bias
33 towards over- or underestimation for that component (Box 1). But what happens when we
34 scale up unbiased predictions to higher levels of organisation? If we do not systematically
35 underestimate the change of individual components, will this still be true when considering
36 many components at once? When addressing this question, one must be wary of basic intuitions
37 as the problem is inherently multi-dimensional, thus hard to properly visualize.

38 As a thought experiment, consider two ecological communities, one species-poor (low dimension)
39 and the other species-rich (high-dimension). Both communities experience perturbations that
40 change species biomass, and we assume that we have an unbiased prediction for this change,
41 up to some level of uncertainty. We then scale up our predictions to the community-level,
42 focusing on the change in Shannon's diversity index, caused by the perturbations. By
43 comparing predicted and observed change we can quantify the degree of underestimation of our
44 predictions, at the species and community-level. If we simulate this thought experiment (Fig. 1
45 and Appendix S4) we observe the following puzzling results, which motivate our subsequent
46 analysis. Predictions of species biomass change may be unbiased (bottom row of Fig. 1), but
47 when scaled up to the system level for the species-rich community, but not the species-poor
48 community, we see a clear bias towards underestimation of change (top right corner of Fig. 1).

49 As we shall explain in depth, the reason for this emergent bias is that *in high dimensions*
50 *there are more ways to be more different, than ways to be more similar*. Our goal is to make
51 this statement quantitative and generally relevant to ecological problems. We start from a
52 geometric approach showing that, in two dimensions, our claim can be visualised to reveal
53 a positive relationship between magnitude of uncertainty and underestimation of change.
54 Visualisation is only possible in low dimensions, but a more abstract reasoning demonstrates
55 that as dimensionality increases so does the bias towards underestimation, which is further

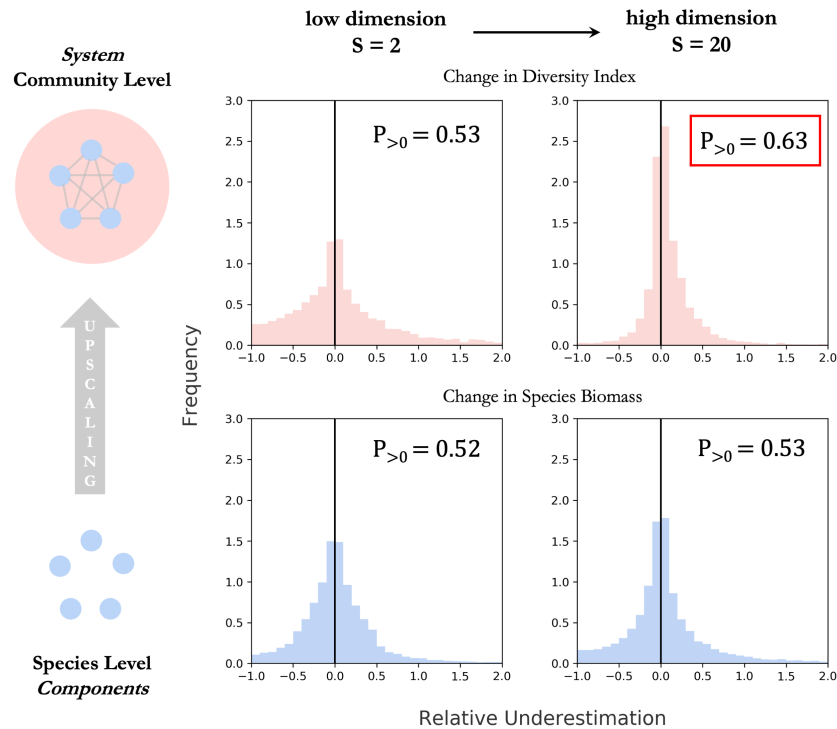


Figure 1: Simulated communities of 2 species (left) and 20 species (right) experienced 1000 perturbations (change in species biomass), for which we assume unbiased predictions at the species-level. Uncertainty around those predictions is simulated as a random terms of zero mean, independent across species. Histograms show the distribution of relative underestimation, defined as the difference between realized and predicted change expressed relatively to the predicted magnitude of change. By construction, there is no bias towards underestimation at the species level (bottom row). We then scale up our predictions to the community level to generate predictions for Shannon’s diversity index (top row). For the first, species poor community, this upscaling does not generate any bias. However, for the species rich community a bias emerges as approximately 75% of realizations show an underestimated magnitude of change. In this article, we explain in depth the statistical mechanisms behind this bias.

56 strengthened by larger uncertainty. We note that dimensionality is not necessarily an integer
 57 value. We propose that the effective dimensionality most relevant to ecological upscaling of
 58 predictions is not the number of species, but instead is a specific diversity metric, the Inverse
 59 Participation Ratio (IPR) (Wegner, 1980; Suweis, Grilli, Banavar, Allesina, & Maritan, 2015),
 60 comparable (but not equivalent) to Hill’s diversity indices (Hill, 1973).

61 We then explain why the effect of dimensionality depends on how change is measured at the
 62 system-level (Box 1). If a single linear function is used to aggregate components (e.g. total
 63 biomass), dimensionality has no effect. An unbiased prediction for individual components
 64 trivially scales up to produce an unbiased system-level prediction. But this is not true in
 65 general. Non-linear functions (e.g. Shannon’s diversity index as in Fig. 1), can remain sensitive
 66 to dimensional effects. Predictions of change of these properties, even if constructed from
 67 unbiased predictions of individual components will be systematically underestimated. The
 68 significance of this effect will depend on the relative significance of non-linearities in the

69 function of interest.

70 On simulated examples we will examine the behaviour of common ecosystem-level properties:
71 diversity, stability and total biomass. More generally, we emphasise that dimensional effects
72 will occur as soon as system-level change is measured as a change in multiple properties at once
73 (whether they are linear or not), as is the case in multi-functional descriptions of ecosystems
74 (Manning et al., 2018).

75 As a seemingly different kind of ecological case-study, we then revisit core questions of multiple-
76 stressor research in the light of our theory. In this field, there is a clear prediction (additivity
77 of stressor effects), a high prevalence of uncertainty about the the way stressors interact
78 (resulting in non-additivity) and, ultimately, great interest in the ecosystem-level consequences
79 of non-additive stressor interactions (synergism or antagonism) (Côté, Darling, & Brown, 2016;
80 Jackson, Loewen, Vinebrooke, & Chimimba, 2016; Piggott, Townsend, & Matthaei, 2015).
81 Expressed in this context, our theory predicts the generation of bias towards synergism when
82 multiple-stressor predictions are scaled up to higher levels of organisation.

83 Research has primarily focused on the causes of uncertainty, working hard to reduce it (Petchey
84 et al., 2015). Here we take a complementary approach by investigating the generic consequences
85 of uncertainty, regardless of the nature of the system studied or the underlying causes of
86 uncertainty. Our theory becomes more relevant as the degree of uncertainty increases, which
87 makes it particularly relevant for ecological problems. But, in fact, our findings could inform
88 any field of science that takes a reductionist approach in the study of complex systems (e.g.
89 economics, energy supply, demography, finance – see Box 2), demonstrating how dimensional
90 effects can play a critical role when scaling up predictions.

91 **2 Geometric Approach**

92 The central claim of this article is that *in high dimensions there are more ways to be more*
93 *different, than ways to be more similar*. We propose an implication: *a system-level predic-*
94 *tion based on unbiased predictions for individual components, will tend to underestimate the*
95 *magnitude of system-level change*.

96 To understand these statements, it is useful to take a geometrical approach to represent the
97 classic reductionist perspective, starting in two dimensions (Fig. 2a). Picture two intersecting
98 circles in a system's state-space (one blue, one red in Fig. 2). The first, blue circle is centred
99 on the system's initial state and its radius corresponds to the predicted magnitude of change.
100 The second, red circle is centred at the predicted state (which lies on the blue circle) and its
101 radius corresponds to the magnitude of realized error of the prediction, in other words, the

Box 1: Lexicon of Concepts

Reductionist view of complex systems

- *Components*: Individual variables B_i that together form a system (e.g. biomass of S species and abiotic compartments forming an ecosystem).
- *System state*: Point in *state space*, represented as a vector $\mathbf{B} = (B_1, \dots, B_S)$ jointly describing all system components.
- *Difference (or magnitude of change) between states*: the Euclidean distance $\|\mathbf{B} - \mathbf{B}'\|$ between two joint states \mathbf{B} and \mathbf{B}' .

Scaling up uncertain predictions

- *Relative error*: Magnitude of error caused by uncertainty relative to the magnitude of predicted change.
- *Aggregate system-level property*: Scalar function of the joint state (e.g. total biomass or diversity index)
 - *Linear aggregate property*: Linear function of joint state variables (e.g. total biomass).
 - *Non-linear property*: Non-linear function of joint state variables (e.g. diversity index).
- *Scaled up prediction*: A prediction made for the joint state, or a scalar property of the joint state, based on individual predictions for components.
- *Unbiased prediction*: A prediction that, despite uncertainties, does not systematically overestimate or underestimate the magnitude of change (of a joint state, a system component or an aggregate property).

Multi-functional view of complex systems

- Multivariate description of a complex system, based on multiple aggregate properties, or *functions* (production, diversity, respiration) instead of individual components (species biomass and abiotic compartments). The state of the system is the joint state $\mathbf{F} = (F_1, \dots, F_{S_F})$ of S_F functions. Difference between states is the distance between two joint functional states \mathbf{F} and \mathbf{F}' .

102 realized outcome of the uncertainty associated with the prediction (red circle in Fig. 2). The
103 actual final state is thus somewhere on that red circle. If it falls outside the blue circle, the
104 prediction has underestimated the magnitude of change. The proportion of the red circle lying
105 outside of the blue circle measures the proportion of possible configurations that will lead
106 to an underestimation of change. In other words, for a given magnitude of error caused by
107 uncertainty, this portion of the circle represents the states that are more different from the
108 initial state than predicted. As the relative magnitude of error increases (as the red circle's
109 diameter becomes larger, relative to that of the blue circle) this proportion grows (Fig. 2a).

110 In three dimensions these two intersecting circles become two intersecting spheres. The
111 proportion of interest is the surface of the spherical cap lying outside of the sphere centred
112 on the initial state. Here, a non-intuitive phenomenon occurs: with the same radii as in the
113 2D case, in 3D there are now more configurations leading to underestimation. As dimensions
114 increase this proportion increases, until the vast majority of possible states now lie in the
115 domain where change is underestimated (Fig. 2b). This result can be made quantitative
116 from known expressions for the surface of hyper-spherical caps. This gives us an analytical
117 expression for the proportion of configurations leading to an underestimation of change, as a
118 function of the relative magnitude of error (x) and dimension (S):

$$P_{>0}(x) = 1 - \frac{1}{2} I_{1-\frac{x^2}{4}} \left(\frac{S-1}{2}; \frac{1}{2} \right); \quad x = \frac{\|\text{error}\|}{\|\text{prediction}\|} \quad (1)$$

119 In the above equations $\|\cdot\|$ stands for the standard Euclidean norm of vectors¹, and $I_s(a, b)$ is
120 the cumulative function of the β -distribution (Appendix S2). This is what we mean by *in high*
121 *dimensions there are more ways to be more different, than ways to be more similar*. To see how
122 this relates to the scaling up of unbiased predictions of individual components (Box 1), we now
123 take a statistical approach. Suppose we uniformly sample the intersecting circles, spheres and
124 hyper-spheres defined above and drawn in Fig. 2. The proportion Eq. (1) becomes a probability,
125 the probability of having underestimated change. This uniform sampling is precisely what
126 happens if the uncertainty of individual variables are independent random normal variables
127 with zero mean (a particular case of an unbiased uncertainty at the component level, see
128 Appendix S2). This justifies our second claim: *a system-level prediction based on unbiased*
129 *predictions for individual components, will tend to underestimate the magnitude of change of*
130 *the system state*.

131 This reasoning is geometrical, and relies on a computation of the surface of classic shapes such
132 as hyper-spheres and spherical caps. But the core mechanism behind the behaviour of the
133 probability of underestimation is more general and in a sense, simpler. To see that, let us take

¹This is the most convenient norm for our geometrical approach but other norms would give similar results.

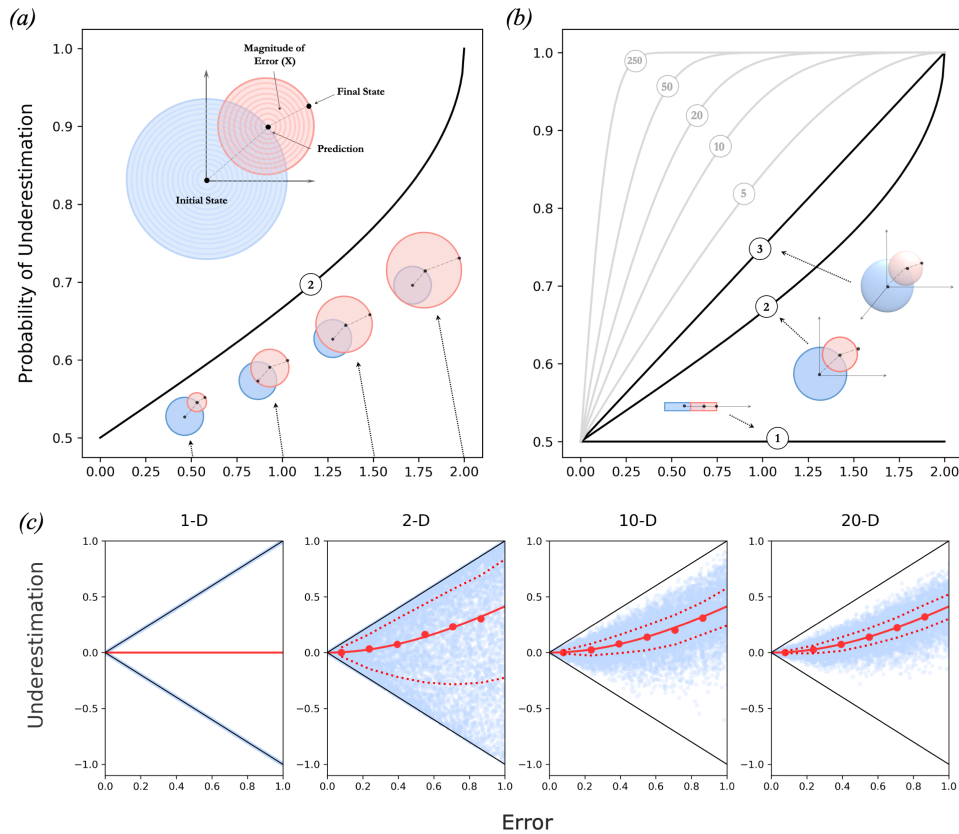


Figure 2: **(a)** Already in two dimensions, the probability of underestimation increases as uncertainty increases. The centre of the blue circle is the initial state (its actual value is irrelevant) and its radius is defined by the predicted magnitude of change. The point at the centre of the red circle corresponds to the predicted state, while its radius represents the magnitude of error made by the prediction. By definition, final states thus fall on the edges of the red circle. If a final state falls inside the blue circle then there has been an overestimation of change (it is closer to the initial state than what was predicted). If a final state falls outside the blue circle (as in the figure) then there has been an underestimation of change (it farther from the initial state than what was predicted). When uncertainty is small, error will be small thus the radius of the red circle is small, and the probability of underestimation is close to 0.5. As uncertainty (thus error) increases, however, there is increasing bias towards underestimation. Eventually when error is twice as large as the prediction only underestimation is possible. **(b)** This relationship between uncertainty and underestimation is strengthened by dimensionality. As dimensions increases there become even more ways to be more different than ways to be more similar. Each curve corresponds to the probability of underestimation as a function of error for different dimensions labeled as circled numbers. For a fixed amount of error the probability of underestimation will increase with dimension. **(c)** The relationship between the relative magnitude of error (x) and the relative magnitude of underestimation (y) based on uniform sampling of 1-D, 2-D, 10-D and 20-D intersecting hyper-spheres defined by unbiased but uncertain predictions. The boundaries of this relationship are plotted in black and the median expectation $\tilde{y} = \sqrt{x^2 + 1} - 1$ as derived from Eq. (4) is plotted in red (except for 1-D where it does not apply). Blue points are simulated results, red points are the actual median values and dashed lines show the quantiles for vertical subsets of the simulated data. As dimensionality increases the width of the distribution decreases and converges towards its median, which effectively increases the probability of underestimation (b).

134 a step back and analyse the relative magnitude of underestimation, defined as:

$$y = \frac{\|\text{response}\| - \|\text{prediction}\|}{\|\text{prediction}\|} \quad (2)$$

135 Given an angle θ between prediction and error vectors (resp. the vectors that point from initial
136 to predicted state, and from predicted state to realized state) we can rearrange Eq. (2) as:

$$y(x, \theta) = \sqrt{x^2 + 2x \cos(\theta) + 1} - 1 \quad (3)$$

137 the term $\cos \theta$ can take any values between -1 and $+1$. For the sake of simplicity, in what
138 follows we will suppose that its mean and median are zero. This is the case if the errors
139 associated with individual variables are drawn from independent symmetric distributions
140 centred on zero (unbiased and unskewed predictions at the component level). In this case the
141 median relationship between error (x) and underestimation (y) is:

$$\tilde{y} = \sqrt{x^2 + 1} - 1 \quad (4)$$

142 which is strictly positive as soon the error x is non zero. This holds true in all dimensions
143 greater than one, which can be seen in Fig. 2c. The median underestimation \tilde{y} does not depend
144 on dimension, but the probability of underestimation, $P(y > 0; x)$, does. Indeed, $P(y > 0; x)$
145 is driven by the distribution of the random term $\cos \theta$ in Eq. (3). If this distribution is narrow,
146 realisations of y will fall close to \tilde{y} . Because the latter is positive and increases predictably
147 with x , so will the probability of any realised y to be positive. A known fact from random
148 geometry is that, given a random isotropic vector (i.e. a vector whose direction is uniformly
149 distributed on the sphere), its angle θ with any other given vector satisfies

$$\mathbb{E}(\cos \theta) = 0; \text{ and } \text{Var}(\cos \theta) = \frac{1}{S} \quad (5)$$

150 In other words, in high dimensions random vectors are approximately orthogonal, up to a
151 variance inversely proportional to the dimension of state-space. In our context, this corresponds
152 to normal i.i.d. distributions of errors, a particular case of independent unbiased and unskewed
153 predictions. This explains why the probability of underestimation increases in Fig. 3b with
154 both dimension S and error x . In what follows we use the expression for the variance in
155 Eq. (5) as a *definition* of *effective dimension*. In doing so, we can free ourselves from the
156 strict Euclidean representation of Fig. 2, and generalize the theory beyond i.i.d. normal error
157 distributions. This will be useful when applying our theory to ecological problems, where
158 components are the biomass of species, are their contribution to ecosystem change are not
159 equivalent, thus errors not i.i.d.

160 3 Relevance to Ecology

161 3.1 Effective Dimensionality

162 We now assume that the axes that define state-space represent the biomass of the species
163 that form an ecological system. These species may have very different abundances, and thus
164 will not all contribute equally to a given change. For instance, in response to environmental
165 perturbations, biomass of species typically change in proportion to their unperturbed values
166 (Lande, Engen, Saether, et al., 2003; Arnoldi, Bideault, Loreau, & Haegeman, 2018). The
167 more abundant species (in the sense of higher biomass) will thus likely contribute more to
168 the ecosystem-level change. Thus, if we use species richness as a measure of dimensionality,
169 as the above section would suggest, we will surely exaggerate the importance of rare (i.e low
170 biomass) species. But using Eq. (5) to *define dimensionality*, we can resolve that issue. In
171 doing so we show that the relevant dimension when applying our ideas to ecological problems
172 is really a measure of diversity of the community prior to the change, which may not be an
173 integer, and will typically be smaller than the number of individual components.

174 In fact (Appendix S3), if a species contribution to change is statistically proportional to its
175 biomass B_i the effective dimensionality of a system is the Inverse Participation Ratio (IPR) of
176 the biomass distribution², which reads:

$$\text{IPR} = \frac{(\sum_{i=1}^S B_i^2)^2}{\sum_{i=1}^S B_i^4} \quad (6)$$

177 This non-integer diversity metric was developed in quantum mechanics to study localisation
178 of electronic states (Wegner, 1980). The IPR approaches 1 when a single species is much
179 more abundant than the others, and approaches S when species have similar abundance – see
180 Suweis *et al.* (2015) where this metric is used in an ecological context. Note that the IPR is
181 closely related (but not equivalent) to Hill (1973)’s evenness measure ${}^2D = (\sum_i B_i)^2 / \sum B_i^2$
182 (see Appendix S3).

183 We can show that it is indeed the IPR that determines the variance (over a sampling of
184 predictions and associated uncertainties of species biomasses) of the term $\cos \theta$ in Eq. (3) so
185 that:

$$\text{Var}(\cos \theta) = \frac{1}{\text{IPR}} \quad (7)$$

186 An uneven biomass distribution thus increases the width of the distribution of underestimation
187 y therefore reducing the probability of a given realisation of change to have been underestimated.

²our theory allows other choices of statistical relationships between biomass and contribution to change, leading to other diversity metrics, which can be seen as generalization of the Inverse Participation Ratio.

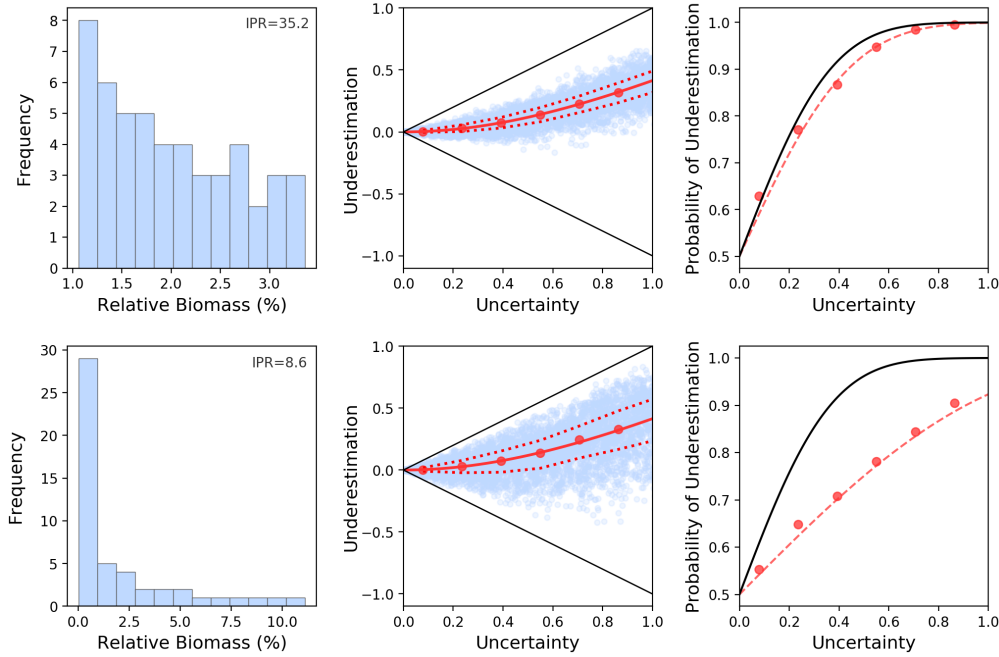


Figure 3: Each row corresponds to simulations of 50 species communities with uneven biomass distributions that have experienced perturbations. The first column shows the biomass distributions of these communities. The two communities have IPR, and therefore effective dimensionality, of 35.2 and 8.6. The second column shows the relationship between error and underestimation of these two communities when unbiased predictions of biomass change are scaled up to change in state-space distance. As the biomass distribution becomes more uneven the variability around the median underestimation increases (dashed lines are quantiles), which effectively reduces the probability that a given change was underestimated. This can be seen in the third column where predictions using the dimension of state-space (50, black curves) are outperformed by predictions using the IPR (35.2 and 8.6, red curves). Red points show the actual probabilities of underestimation for vertical subsets of the simulated data and are accurately predicted using the IPR.

188 If species richness accurately predicted the width of the distribution of underestimation and
 189 therefore the probability of underestimation, the two simulated communities in Fig. 3 would
 190 behave in the same way. However, the probability of underestimation is lower than expected
 191 based on richness, particularly for the community with a more uneven biomass distribution.
 192 Indeed, replacing richness S by the IPR in Eq. (1) provides an excellent approximation of the
 193 behaviour of the probability of underestimation (Fig. 3).

194 3.2 Aggregate Properties and Non-Linearity

195 When scaling up predictions, there are different ways of measuring system-level change (Box 1).
 196 The classic reductionist approach is to quantify change via the Euclidean distance in state-
 197 space, thus keeping track of the motion of joint configurations. This is what we have done
 198 so far. Ecologically, this could correspond to measuring the absolute biomass change of a
 199 community. Here, by construction, our theory is directly relevant.

200 But other, non reductionist, ways of quantifying change at the system-level are possible. In

201 ecology, this could correspond to measuring changes in the diversity, stability or functioning
202 of the ecosystem. Yet, if differences in these properties between two states correlate with the
203 distance in the reductionist state-space, then our theory will remain relevant. As can be seen
204 in Fig. 4 this can be the case for diversity (Shannon’s index) and stability (invariability of
205 total biomass (Haegeman et al., 2016)). Our theory thus applies to those ecosystem-level
206 properties. This leads us to the conclusion that their degree of change will be systematically
207 underestimated by predictions built from species-level predictions.

208 On the other hand, changes of total biomass (ecosystem functioning) do not correlate well
209 with changes in state-space Euclidean distance. This is due to the fact that total biomass is a
210 linear function of species biomass (i.e. the sum). In fact, quantifying system-level change via a
211 linear function acts as a projection from the state space onto a one-dimensional space defined
212 by the function. Thus, despite the fact that the ecosystem might be constituted of many
213 species (intrinsically high dimensional) the problem of scaling up predictions is essentially one
214 dimensional. This is why bottom-up predictions of change of total biomass show no additional
215 bias towards underestimation.

216 More generally, when the linear part of the aggregate property of interest is dominant,
217 dimensional effects are obscured. However, as soon as we consider changes of multiple
218 properties at once, as in multi-functionality approaches in ecology (Box 1), dimensional effects
219 will play out – even if all aggregate properties are essentially linear.

220 **3.3 Multi-Functionality**

221 Scaling up predictions from individual components to an aggregate property can lead to a
222 bias towards underestimation, due to dimensional effects. We explained that this occurs for
223 non-linear aggregate properties, and not linear ones (such as total biomass). Is this to say that
224 our theory is only relevant when predicting the change of non-linear system-level properties?
225 Yes, but only in the restricted realm of one-dimensional approaches to complex systems.

226 There is, in ecology, a growing interest in multi-functionality approaches (Manning et al.,
227 2018). These approaches are multivariate descriptions of ecosystems, an alternative to the
228 reductionist perspective to account for the multidimensional nature of ecological systems
229 (Box 1). By considering the change of multiple functions at once, even if these functions are
230 essentially linear, dimensional effects will resurface.

231 To be clear, we still assume that we scale up predictions from the species to the ecosystem
232 level. Only now we scale up predictions from species to several system-level properties at once,
233 that describe the ecosystem’s state from a multi-functional point of view (Box 1). Let us
234 suppose, for simplicity, that those aggregate properties (or functions) are essentially linear.

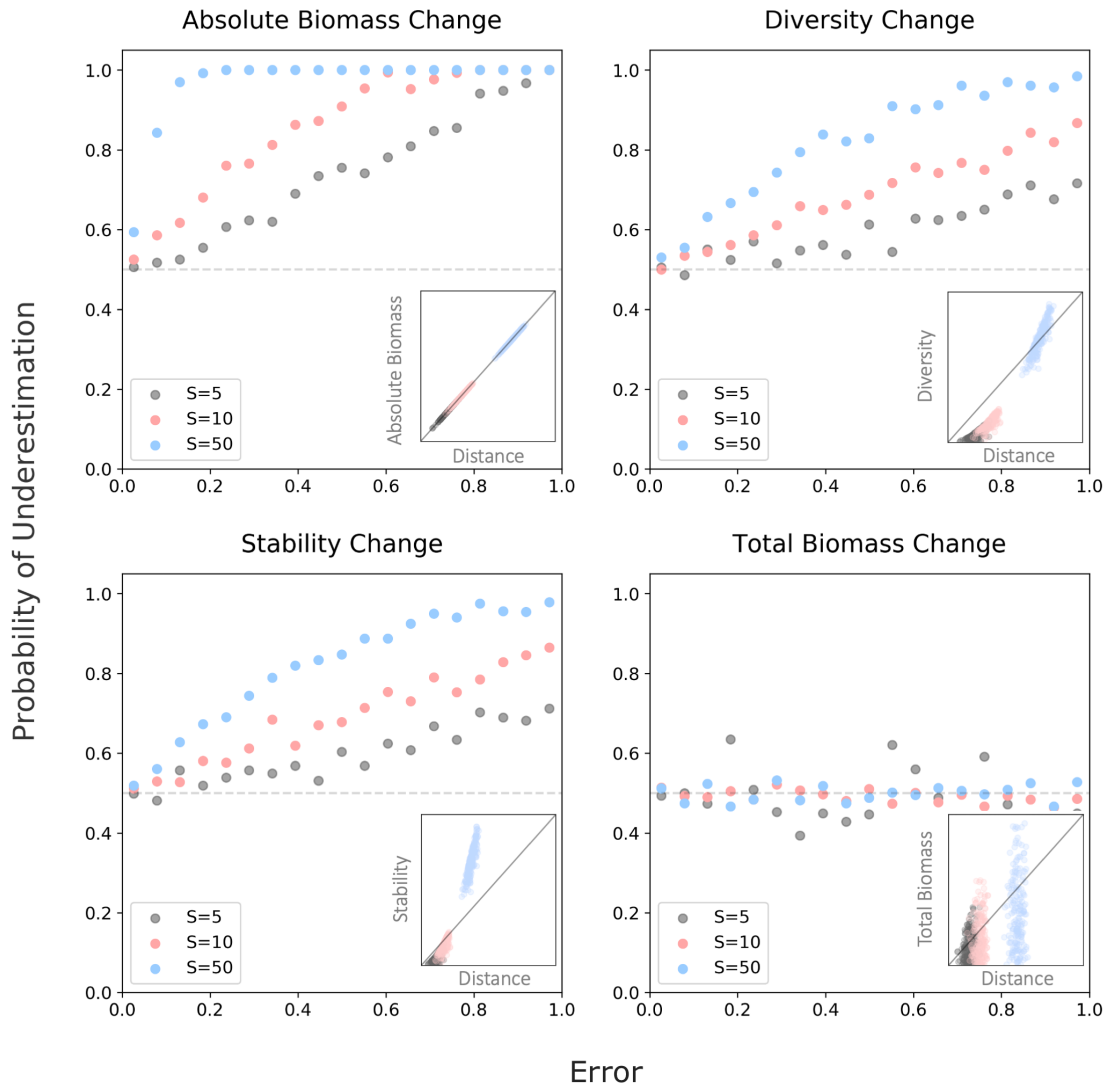


Figure 4: Simulated communities of 5 (grey), 10 (red) and 50 (blue) species experienced some change in their biomass. Unbiased predictions of species' biomass change were scaled up to predictions of change in aggregate properties commonly used in ecological research. The relationship between uncertainty and the probability of underestimation is shown for changes in: (1) absolute biomass, (2) diversity, specifically the Shannon index, (3) stability, specifically invariability and (4) total biomass. Subplots show the relationship between changes in each aggregate property and changes in Euclidean distance. Absolute biomass change is analogous to Euclidean distance. Diversity and stability (non-linear functions) show some correlation with Euclidean distance and are therefore sensitive to dimensional effects. Total biomass (linear function) does not correlate with Euclidean distance so scaled up predictions of change of this aggregate property remain unbiased.

235 We have seen that considering a single linear function, in terms of upscaling of predictions,
 236 essentially reduces the problem to a single dimension. Likewise, considering multiple linear
 237 functions essentially reduces the effective dimensionality to the number of functions. Subtleties
 238 arise when the number of functions (S_f) and the dimensionality of the underlying system (e.g.
 239 IPR) are similar, and/or if the considered functions are colinear (see Appendix S3). For S_f
 240 independent functions measured on a community we find that the effective dimensionality (the

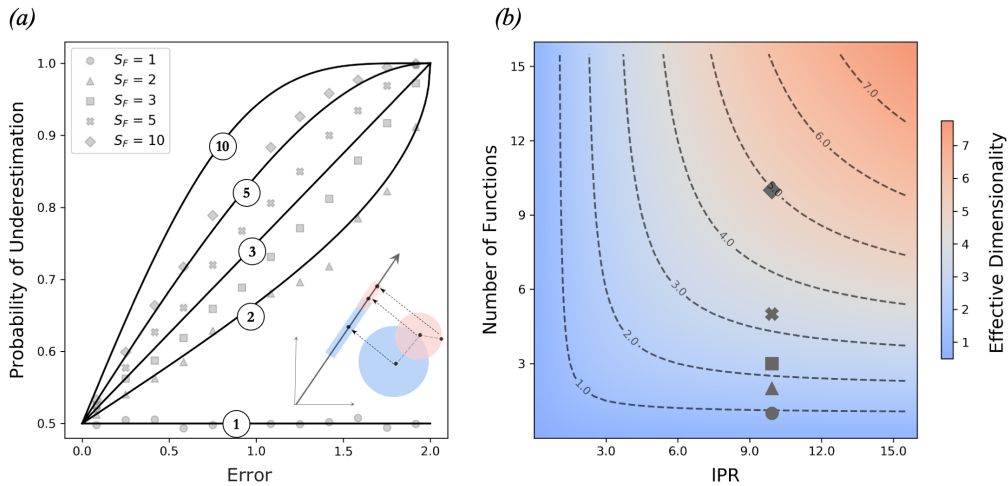


Figure 5: **(a)** The relationship between prediction error caused by uncertainty and the probability of underestimation for five simulations each scaling up predictions to a different number of aggregate properties (S_F). A community of 20 species, with IPR of 9.9, experienced change in biomass over 50,000 simulations. Unbiased predictions at the species level were scaled up to the community level using 1, 2, 3, 5 and 10 randomly drawn aggregate properties. Simulated results fall short of theoretical expectations for the probability of underestimation when the effective dimensionality is presumed to be the number of functions. The blue and red circles being projected onto a blue and red line represents a 2-D system being projected into 1-D functional space. **(b)** There is an interaction between the number of functions and the underlying dimensionality (IPR), which is illustrated by the heat-map. Usually the effective dimensionality is determined by the lower value of S_F and IPR. However, when these values are similar (e.g. diamond: 10 functions and IPR of 9.9) the effective dimensionality (~ 5) is much lower than either value.

241 one that determines the probability of underestimation of change) is:

$$S_{\text{eff}} \approx \frac{1}{\frac{1}{\text{IPR}} + \frac{1}{S_f}} \quad (8)$$

242 For example, if the change of an ecosystem with an IPR of 10 is measured using 10 linear
 243 functions at once, the effective dimensionality is ~ 5 (Fig. 5). If functions are colinear the
 244 effective dimensionality will be even lower than S_f . This is to be expected, especially when
 245 thinking of an extreme case: if we measure the same function multiple times we should see no
 246 dimensional effects. In summary, in a multivariate description of complex systems, dimensional
 247 effects will inevitably play out, in more or less intricate ways, whenever a prediction is scaled
 248 up from individual components to the system-level.

249 4 Discussion

250 Our work demonstrates that a bias towards underestimation of change emerges when predictions
 251 of individual components (e.g. species biomass) are scaled up to the system-level (e.g. ecosystem
 252 function). Our geometric approach reveals a direct relationship between the probability of
 253 underestimation, the magnitude of error caused by uncertainty and a system's effective

254 dimensionality. We noted that the effective dimensionality is not necessarily the number of
 255 individual components that form a system, but rather a measure of diversity *sensu* Hill (1973).
 256 In essence, these results come from the fact that *in high dimensions there are more ways to*
 257 *be more different, than ways to be more similar* (Fig. 6). Our goal was to make this remark
 258 quantitative and generally relevant to ecological problems.

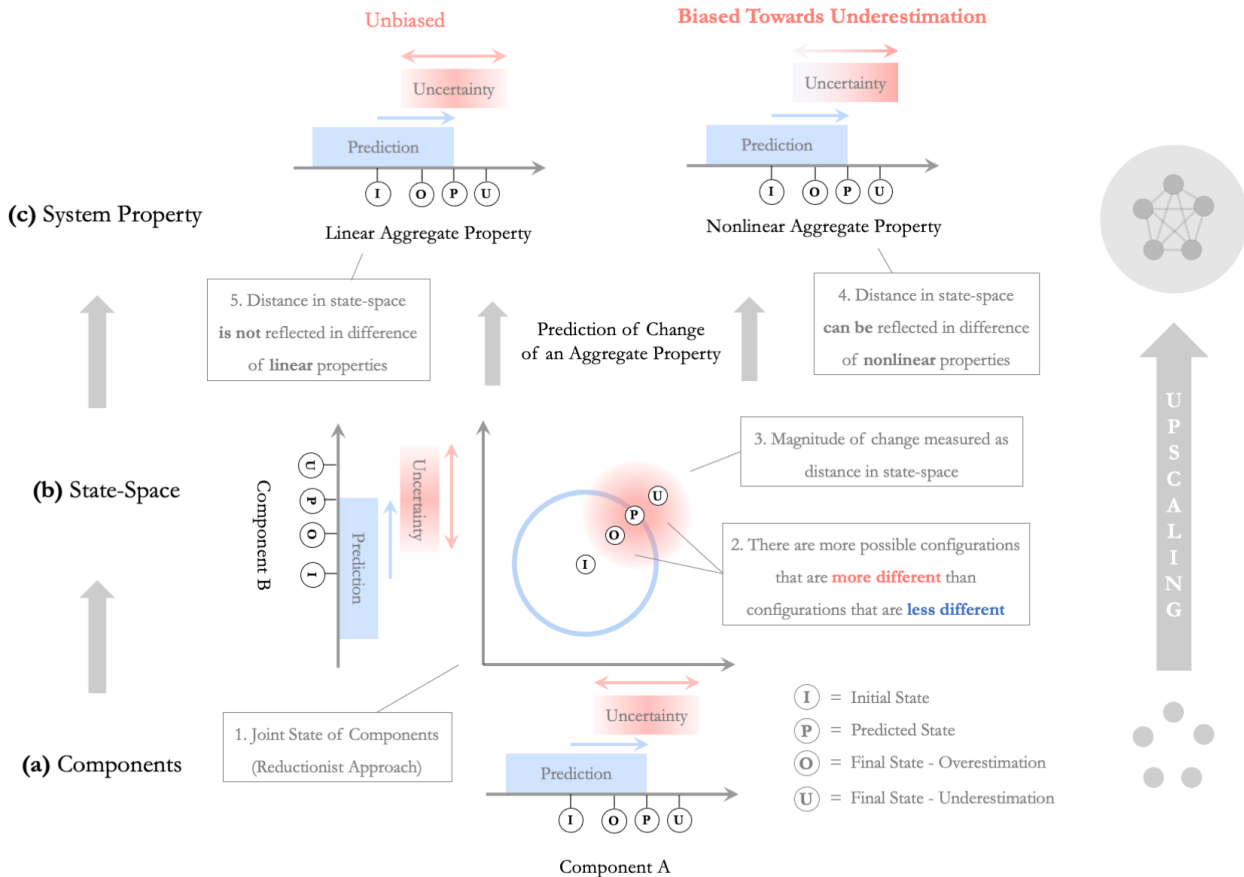


Figure 6: An overview of our main findings. **(a)** Two components, A and B are **(b)** considered at once to define a joint state (I). Suppose this state changes and falls near a predicted state (P). Then there are more ways for this state to be more different from (I), than ways to be more similar; more of the red disk is outside the blue circle than inside. Consequently, when predictions of change (blue) for individual components are scaled up to predictions of change of their joint state, unbiased uncertainties (red) become biased towards underestimation. In section *Geometric Approach* we quantified these surprising dimensional effects and investigate beyond the basic two-dimensional case shown here. **(c)** Magnitude of system-level change can be measured as distance in state space or by some other aggregate property. If an aggregate property is sensitive to changes in distance of the underlying state-space, dimensional effects, and therefore a bias towards underestimation, will be conserved. As we explained in section *Aggregate Properties and Non-Linearity*, it is the non-linear part of an aggregate property that controls its sensitivity to changes in state-space distance and thus the tendency of its degree of change to be underestimated by upscaled predictions.

259 We explained why it is non-linear aggregate properties (e.g. absolute biomass change, stability
 260 or diversity) that are sensitive to dimensional effects (Fig. 6). For linear properties (e.g. total
 261 biomass), scaling up does not generate bias. Yet, even in this case, dimensional effects will play

262 out if several functions are considered at once to describe the ecosystem, as in multi-functional
263 approaches in ecology.

264 Natural systems are intrinsically complex and the way that we describe them is necessarily
265 multivariate (Loreau, 2010). It is generally accepted, in ecology, that there is a need for
266 mechanistic predictive models, built from individual components and scaled up to the ecosystem-
267 level (Poff, 1997; Mouquet et al., 2015; Harfoot et al., 2014; Woodward et al., 2010). We
268 have shown that dimensional effects will play out in this scaling-up, generating additional bias
269 towards underestimation of any predicted system-level change. This is not to say that scaling
270 up predictions is a faulty approach, rather that one must keep track of dimensional effects
271 when doing so.

272 Our theory provides a generic expectation for the consequences of uncertainty when predictions
273 are scaled up from individual components to the system as a whole. As a result, it provides
274 a baseline, of what to expect if only dimensional effects are at play, against which we can
275 test biological (or other) effects. To inform empirical work, it is important to recognise that
276 there are two ways that a result can deviate from our generic expectation. Focusing on the
277 relationship between uncertainty and underestimation of change shown in Figs. 2-3, the median
278 can be shifted due to a systematic bias caused by interactions between component uncertainties,
279 which are assumed independent and in our framework. Furthermore, the distribution around
280 this median can be more than or less than expected, which indicates either wrong estimation
281 of effective dimensionality, or a systematic effect caused by something other than geometry
282 (e.g. skewed distributions of errors or interactions). Having a clear baseline against which to
283 identify non-geometric effects can improve our understanding of complex systems.

284 We only considered two levels of organisation: the level where predictions are made and the
285 level where predictions are scaled up to. However, intermediate levels could, in principle,
286 be considered. For instance, given the increasing resolution of ecological data, predictions
287 of change may originally be based at the level of individual organisms and could first be
288 scaled up to species-level predictions and subsequently scaled up to ecosystem-level predictions.
289 Here, if non-linear aggregate properties are used, dimensional effects will bias species-level
290 predictions towards underestimation and will further increase this bias for ecosystem-level
291 predictions. With an ever-increasing resolution of data, scaling predictions across multiple
292 levels of organisation, and potentially introducing dimensional effects at multiple levels, may
293 become more common in the study of complex systems.

294 Our work is theoretical and, in essence abstract. Yet it may be relevant for highly practical
295 domains of ecology. To make this point, we will now discuss some implications of our theory
296 to multiple-stressor ecological research, an essentially empirical field that explicitly deals with

297 considerable uncertainty of predictions and holds great interest in its consequences.

298 **4.1 Multiple-Stressor Research**

299 In the light of our theory, we propose to revisit a seemingly unrelated problem of wide ecological
300 interest: what is the combined effect of multiple stressors on a given ecosystem? By translating
301 our theory into the language of multiple-stressor research we aim to highlight some implications
302 and to inspire further generalization.

303 The combined effect of stressors on an ecological system is generally predicted based on the sum
304 of their isolated effects, i.e. an “additive null model” (Folt, Chen, Moore, & Burnaford, 1999;
305 Schäfer & Piggott, 2018). Uncertainty around this additive prediction, which is ubiquitous
306 in empirical studies (Crain, Kroeker, & Halpern, 2008; Jackson et al., 2016; Holmstrup
307 et al., 2010), causes prediction errors called “non-additivity”. Uncertain predictions will
308 either overestimate or underestimate the combined effect of stressors, respectively creating
309 “antagonism” and “synergism” (Folt et al., 1999; Piggott et al., 2015). This translation of
310 stressor interactions in terms of prediction uncertainty and under- or over-estimation lead
311 us to the conclusion that scaling up uncertain multiple-stressor predictions generates bias
312 towards synergism.

313 Here, scaling up predictions refers to multiple-stressor predictions (e.g. an additive model)
314 at one level (e.g., individuals, populations) being used to build multiple-stressor predictions
315 at higher levels of biological organisation (e.g. communities, ecosystems), an approach for
316 which there is growing interest (Orr et al., 2020; Thompson, MacLennan, & Vinebrooke, 2018;
317 Kroeker, Kordas, & Harley, 2017; Côté et al., 2016). To be clear, scaling up predictions is not
318 equivalent to simply scaling up investigations; our theory does not predict greater synergism
319 at higher levels of organisation. In fact, we are not making predictions about how stressors
320 will behave at higher levels of organization. What we claim instead is that, if we have a model
321 for the combined effect of stressors at one level of organization and use that model to deduce
322 their combined effect at higher levels, the process of scaling up the model will introduce a bias
323 towards an observed synergy between stressors, even if no systematic synergy was observed at
324 the lower level.

325 Our theory has consequences for the interpretation of stressor interactions and is therefore
326 relevant to the debate surrounding multiple-stressor null models (Griffen, Belgrad, Cannizzo,
327 Knotts, & Hancock, 2016; Liess, Foit, Knillmann, Schäfer, & Liess, 2016; De Laender, 2018;
328 Schäfer & Piggott, 2018). Our findings are especially relevant to the *Compositional Null Model*,
329 which employs a reductionist approach to the construction of multiple-stressor predictions
330 (Thompson et al., 2018). In such an approach, the baseline against which biological effects are

331 tested must be shifted. Dimensional effects, quantified by the effective dimensionality of the
332 underlying system and the non-linearity of aggregate properties, need to be accounted for to
333 decipher a biological synergism from merely a statistical synergism.

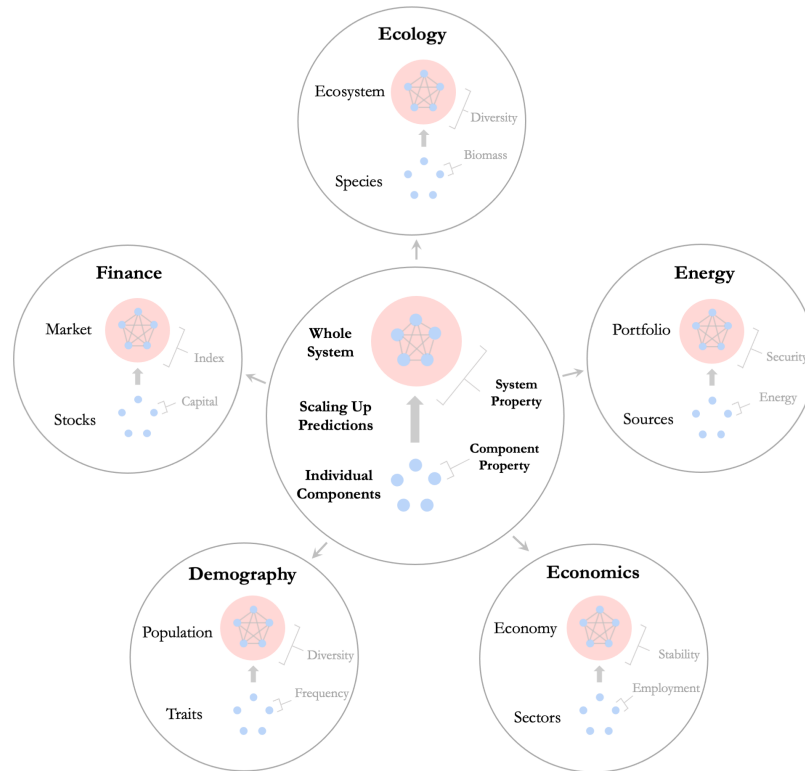
334 **4.2 Conclusions**

335 In this paper we have addressed a subproblem of the reductionist program (Levins & Lewontin,
336 1985; Wan, 2013; Loreau, 2010). We investigated the consequences of uncertainty when
337 unbiased predictions of individual components are scaled up to predictions of system-level
338 change. Due to a geometric observation that *in high dimensions there are more ways to be more*
339 *different, than ways to be more similar*, scaling up uncertain predictions can underestimate
340 system-level change. These dimensional effects manifest when non-linear, but not linear,
341 aggregate properties are used to measured change at the system level, and when multiple
342 functions are considered at once. Although we have primarily focused on ecology, and in
343 particular on the response of ecosystems to perturbations; our general findings could inform any
344 field of science where predictions about whole systems are constructed from joint predictions
345 on their individual components, such as economics, finance, energy supply, and demography
346 (Box 2).

347 **Acknowledgements**

348 We thank Matthieu Barbier, Nuria Galiana and Yuval Zelnik for discussions and review of
349 previous versions of this work. JFA and ALJ were supported by an Irish Research Council
350 Laureate Award IRCLA/2017/186. JO was supported by an Irish Research Council Laureate
351 Award IRCLA/2017/112 and TCD Provost's PhD Award held by JP.

Box 2: Generalisation Beyond Ecology



Our findings could be relevant to other fields of science where: (i) there is interest in predicting change of complex systems based on knowledge about their individual components, and (ii) systems are described using multivariate coordinates and/or using non-linear properties of individual components.

- In **economics**, a region's economy can be viewed as a complex system comprised of individual sectors (e.g. agriculture, tourism, technology). Predictions of how employment numbers will change in individual sectors due to some perturbation could be scaled up to predictions of change of economy-level properties of interest such as stability, measured as, for example, the evenness of employment across sectors (Halpern et al., 2012; Malizia & Ke, 1993; Dissart, 2003).
- In the study of **energy supply**, different fuel or energy sources of a country (e.g. solar, wind, oil) can be considered together in a country's energy portfolio. Predictions of change of energy generation in each individual source could be scaled up to predictions of change of portfolio-level properties. Energy security is a system-level property of great interest that is quantified using diversity metrics (Stirling, 1994; Chalvatzis & Ioannidis, 2017) or variance-based approaches (Roques, Newbery, & Nuttall, 2008) based on *Mean-Variance Portfolio Theory*, which was originally developed to study risk or volatility of investment portfolios (Markowitz & Todd, 2000).
- In **demography**, populations can be thought of as systems comprised of multiple different groups that are defined by traits (e.g. gender, age, ethnicity). Again, diversity is a system-level property of great interest in the study of populations that is quantified using non-linear aggregate functions (Reardon & Firebaugh, 2002; White, 1986). Changes in diversity of human populations is pertinent to many social sciences including **sociology, economics and politics**.
- In **finance**, markets are complex systems whose individual components are stocks. Predictions of how the capital of individual stocks will change could be scaled up to predictions of how stock market indices will change. Certain stock market indices, for example diversity-weighted indices, are non-linear aggregate properties that will be sensitive to dimensional effects (Fernholz, Garvy, & Hannon, 1998; Chow, Hsu, Kalesnik, & Little, 2011). At a different financial scale, our theory may also be relevant to the study of investment portfolios. Here, analogous to energy security, portfolios are systems comprised of individual assets and the volatility or risk tolerance of a portfolio (measured using non-linear aggregate properties) is of great interest to investors (Markowitz & Todd, 2000; Bera & Park, 2008).

References

- 353 Arnoldi, J.-F., Bideault, A., Loreau, M., & Haegeman, B. (2018). How ecosystems recover from
354 pulse perturbations: A theory of short-to long-term responses. *Journal of theoretical*
355 *biology*, *436*, 79–92.
- 356 Bera, A. K., & Park, S. Y. (2008). Optimal portfolio diversification using the maximum
357 entropy principle. *Econometric Reviews*, *27*(4-6), 484–512.
- 358 Chalvatzis, K. J., & Ioannidis, A. (2017). Energy supply security in the eu: Benchmarking
359 diversity and dependence of primary energy. *Applied Energy*, *207*, 465–476.
- 360 Chow, T.-m., Hsu, J., Kalesnik, V., & Little, B. (2011). A survey of alternative equity index
361 strategies. *Financial Analysts Journal*, *67*(5), 37–57.
- 362 Côté, I. M., Darling, E. S., & Brown, C. J. (2016). Interactions among ecosystem stressors
363 and their importance in conservation. *Proceedings of the Royal Society B: Biological*
364 *Sciences*, *283*(1824), 20152592.
- 365 Crain, C. M., Kroeker, K., & Halpern, B. S. (2008). Interactive and cumulative effects of
366 multiple human stressors in marine systems. *Ecology Letters*, *11*(12), 1304–1315.
- 367 De Laender, F. (2018). Community-and ecosystem-level effects of multiple environmental
368 change drivers: Beyond null model testing. *Global Change Biology*, *24*(11), 5021–5030.
- 369 Dissart, J. C. (2003). Regional economic diversity and regional economic stability: research
370 results and agenda. *International Regional Science Review*, *26*(4), 423–446.
- 371 Dovers, S. R., & Handmer, J. W. (1992). Uncertainty, sustainability and change. *Global*
372 *Environmental Change*, *2*(4), 262–276.
- 373 Fernholz, R., Garvy, R., & Hannon, J. (1998). Diversity-weighted indexing. *Journal of*
374 *Portfolio Management*, *24*(2), 74.
- 375 Folt, C., Chen, C., Moore, M., & Burnaford, J. (1999). Synergism and antagonism among
376 multiple stressors. *Limnology and Oceanography*, *44*(3part2), 864–877.
- 377 Griffen, B. D., Belgrad, B. A., Cannizzo, Z. J., Knotts, E. R., & Hancock, E. R. (2016).
378 Rethinking our approach to multiple stressor studies in marine environments. *Marine*
379 *Ecology Progress Series*, *543*, 273–281.
- 380 Haegeman, B., Arnoldi, J.-F., Wang, S., de Mazancourt, C., Montoya, J. M., & Loreau, M.
381 (2016). Resilience, invariability, and ecological stability across levels of organization.
382 *bioRxiv*, 085852.
- 383 Halpern, B. S., Longo, C., Hardy, D., McLeod, K. L., Samhouri, J. F., Katona, S. K., ...
384 others (2012). An index to assess the health and benefits of the global ocean. *Nature*,
385 *488*(7413), 615–620.
- 386 Harfoot, M. B., Newbold, T., Tittensor, D. P., Emmott, S., Hutton, J., Lyutsarev, V., ...
387 Purves, D. W. (2014). Emergent global patterns of ecosystem structure and function

- 388 from a mechanistic general ecosystem model. *PLoS Biology*, 12(4).
- 389 Hill, M. O. (1973). Diversity and evenness: A unifying notation and its consequences. *Ecology*,
390 54(2), 427-432. doi: 10.2307/1934352
- 391 Holmstrup, M., Bindsbøl, A.-M., Oostingh, G. J., Duschl, A., Scheil, V., Köhler, H.-R., ...
392 others (2010). Interactions between effects of environmental chemicals and natural
393 stressors: a review. *Science of the Total Environment*, 408(18), 3746-3762.
- 394 Jackson, M. C., Loewen, C. J., Vinebrooke, R. D., & Chimimba, C. T. (2016). Net effects
395 of multiple stressors in freshwater ecosystems: a meta-analysis. *Global Change Biology*,
396 22(1), 180-189.
- 397 Kroeker, K. J., Kordas, R. L., & Harley, C. D. (2017). Embracing interactions in ocean
398 acidification research: confronting multiple stressor scenarios and context dependence.
399 *Biology Letters*, 13(3), 20160802.
- 400 Lande, R., Engen, S., Saether, B.-E., et al. (2003). *Stochastic population dynamics in ecology*
401 *and conservation*. Oxford University Press on Demand.
- 402 Levins, R., & Lewontin, R. C. (1985). *The dialectical biologist*. Harvard University Press.
- 403 Liess, M., Foit, K., Knillmann, S., Schäfer, R. B., & Liess, H.-D. (2016). Predicting the
404 synergy of multiple stress effects. *Scientific Reports*, 6, 32965.
- 405 Loreau, M. (2010). *From populations to ecosystems: Theoretical foundations for a new*
406 *ecological synthesis (mpb-46)* (Vol. 46). Princeton University Press.
- 407 Malizia, E. E., & Ke, S. (1993). The influence of economic diversity on unemployment and
408 stability. *Journal of Regional Science*, 33(2), 221-235.
- 409 Manning, P., van der Plas, F., Soliveres, S., Allan, E., Maestre, F. T., Mace, G., ... Fischer,
410 M. (2018). Redefining ecosystem multifunctionality. *Nature Ecology & Evolution*, 2(3),
411 427-436.
- 412 Markowitz, H. M., & Todd, G. P. (2000). *Mean-variance analysis in portfolio choice and*
413 *capital markets* (Vol. 66). John Wiley & Sons.
- 414 Mouquet, N., Lagadeuc, Y., Devictor, V., Doyen, L., Duputié, A., Eveillard, D., ... others
415 (2015). Predictive ecology in a changing world. *Journal of Applied Ecology*, 52(5),
416 1293-1310.
- 417 Orr, J. A., Vinebrooke, R. D., Jackson, M. C., Kroeker, K. J., Kordas, R. L., Mantyka-Pringle,
418 C., ... others (2020). Towards a unified study of multiple stressors: divisions and
419 common goals across research disciplines. *Proceedings of the Royal Society B*, 287(1926),
420 20200421.
- 421 Petchey, O. L., Pontarp, M., Massie, T. M., Kéfi, S., Ozgul, A., Weilenmann, M., ... others
422 (2015). The ecological forecast horizon, and examples of its uses and determinants.
423 *Ecology Letters*, 18(7), 597-611.
- 424 Piggott, J. J., Townsend, C. R., & Matthaei, C. D. (2015). Reconceptualizing synergism and

- 425 antagonism among multiple stressors. *Ecology and Evolution*, 5(7), 1538–1547.
- 426 Poff, N. L. (1997). Landscape filters and species traits: towards mechanistic understanding
427 and prediction in stream ecology. *Journal of the North American Benthological Society*,
428 16(2), 391–409.
- 429 Reardon, S. F., & Firebaugh, G. (2002). Measures of multigroup segregation. *Sociological*
430 *Methodology*, 32(1), 33–67.
- 431 Roques, F. A., Newbery, D. M., & Nuttall, W. J. (2008). Fuel mix diversification incentives
432 in liberalized electricity markets: A mean–variance portfolio theory approach. *Energy*
433 *Economics*, 30(4), 1831–1849.
- 434 Schäfer, R. B., & Piggott, J. J. (2018). Advancing understanding and prediction in multiple
435 stressor research through a mechanistic basis for null models. *Global Change Biology*,
436 24(5), 1817–1826.
- 437 Stirling, A. (1994). Diversity and ignorance in electricity supply investment: Addressing the
438 solution rather than the problem. *Energy Policy*, 22(3), 195–216.
- 439 Suweis, S., Grilli, J., Banavar, J. R., Allesina, S., & Maritan, A. (2015). Effect of localization
440 on the stability of mutualistic ecological networks. *Nature Communications*, 6, 10179.
- 441 Thompson, P. L., MacLennan, M. M., & Vinebrooke, R. D. (2018). An improved null model
442 for assessing the net effects of multiple stressors on communities. *Global Change Biology*,
443 24(1), 517–525.
- 444 Wan, P. Y.-z. (2013). Dialectics, complexity, and the systemic approach: Toward a critical
445 reconciliation. *Philosophy of the Social Sciences*, 43(4), 411–452.
- 446 Wegner, F. (1980). Inverse participation ratio in $2+ \varepsilon$ dimensions. *Zeitschrift für Physik B*
447 *Condensed Matter*, 36(3), 209–214.
- 448 White, M. J. (1986). Segregation and diversity measures in population distribution. *Population*
449 *Index*, 198–221.
- 450 Woodward, G., Perkins, D. M., & Brown, L. E. (2010). Climate change and freshwater
451 ecosystems: impacts across multiple levels of organization. *Philosophical Transactions*
452 *of the Royal Society B: Biological Sciences*, 365(1549), 2093–2106.
- 453 Wu, J., Jones, B., Li, H., & Loucks, O. L. (2006). *Scaling and uncertainty analysis in ecology*.
454 Springer.

455

456

Supporting Information

457

James Orr, Jeremy Piggott, Andrew Jackson, and Jean-François Arnoldi

458

S1 Geometrical model

459

Consider a complex system whose states are given by points in \mathbb{R}^S (thus determined by S individual variables, e.g species biomass). Let $v \in \mathbb{R}^S$ be an expectation for a change of state.

460

461

Let w be the actual change that is observed, and define the error vector u such that $w = v + u$.

462

From u and v we define a scalar measure x of relative error as

$$x = \frac{\|u\|_2}{\|v\|_2}$$

463

We formalize the question of whether there has been more change observed than predicted, by

464

defining

$$y = \frac{\|w\|_2 - \|v\|_2}{\|v\|_2}$$

465

In both of the above expressions $\|\cdot\|_p$ denotes the L_p norm of vectors. $p = 2$ corresponds to

466

Euclidean distance, we still see below that other values of p can occur in our formalism. Also,

467

our results hold for other choices of norm in defining x and y . The Euclidian norm is however,

468

the most convenient for a geometrical approach. A reorganization of y gives

$$y = y(x, \theta) = \sqrt{1 + x^2 + 2x \cos \theta} - 1$$

469

where θ is the angle between error u and prediction v , that is

$$\cos \theta = \frac{\langle u|v \rangle}{\|u\|_2 \|v\|_2}$$

470

S2 Random ensemble

471

We now assume that u and v are random variables (but the prediction v could also be given).

472

We assume however that the components of u_i have zero mean and median – the prediction

473

of individual variables is unbiased and unskewed. Then $\mathbb{E}_u \langle u|v \rangle = 0$, thus $\mathbb{E} \cos \theta = 0$. This

474 implies that

$$\mathbb{M}_u y = \sqrt{1 + x^2} - 1$$

475 At fixed error x , the distribution around this median is driven by variance of $\cos \theta$, over random
 476 draws of vectors u and v . We first define the covariance matrices $C^u = (C_{ij}^u) = \mathbb{E}_u (u_i u_j)$, and
 477 $C^v = (C_{ij}^v) = \mathbb{E}_v (v_i v_j)$. We then have that

$$\begin{aligned} \mathbb{E}_{u,v} \langle u|v \rangle^2 &= \mathbb{E}_{u,v} \langle v|u \rangle \langle u|v \rangle \\ &= \mathbb{E}_v \langle v|C^u v \rangle \\ &= \text{Tr} C^u C^v \end{aligned}$$

478 and similarly

$$\mathbb{E}_{u,v} \|u\|^2 \|v\|^2 = \text{Tr} C^u \text{Tr} C^v$$

479 Thus

$$\mathbb{E} \cos^2 \theta \simeq \frac{\text{Tr} C^u C^v}{\text{Tr} C^u \text{Tr} C^v} \quad (\text{S1})$$

480 Example

481 Suppose that $C_u = \sigma^2 \mathbb{I}$ where \mathbb{I} is the identity matrix. This implies that uncertainties of the
 482 individual variables are independent random variables with variance σ^2 . We then have

$$\mathbb{E}_u \langle u|v \rangle^2 = \sigma^2 \|v\|^2$$

483 while

$$\mathbb{E}_u \|u\|^2 = S \sigma^2$$

484 so that

$$\mathbb{E}_u \cos^2 \theta \simeq \frac{1}{S}$$

485 S2.1 Probability of underestimation

486 Given an imprecision level x , the theory has underestimated the actual response if $y(x, \theta) \geq 0$
 487 and thus if the angle θ between the theoretical prediction v and the vector of unaccounted
 488 change u satisfies

$$\cos \theta \geq -\frac{x}{2}$$

489 If $\cos \theta$ is approximately normally distributed with zero mean and variance $\sigma^2 = \frac{1}{S}$, than

$$\mathbb{P}(y \geq 0 : x) \simeq \frac{1}{\sqrt{2\pi\sigma^2}} \int_{-\frac{x}{2}}^{\infty} \exp\left(-\frac{s^2}{2\sigma^2}\right) ds$$

490 hence, by the properties of the cumulative distribution function of standard normal distributions,
 491 one gets

$$\mathbb{P}(y \geq 0 : x) \simeq \frac{1}{2} \left[1 + \operatorname{erf} \left(\frac{x}{2} \sqrt{\frac{S}{2}} \right) \right]$$

492 where erf is the error function. This expression should be compared to the exact solution
 493 in the case of a uniform sampling over the direction of u (which is the case if $u_i \sim \mathcal{N}(0, 1)$
 494 –uncertainties of individual variables are independent and normally distributed). In this special
 495 case the problem of deriving the probability of underestimation becomes purely geometrical:
 496 it is the surface of a ball of radius x and centered on the unit sphere, that is contained in the
 497 unit ball. One then gets

$$\mathbb{P}(y \geq 0 : x) = 1 - \frac{1}{2} I_{1-\frac{x^2}{2}} \left(\frac{S-1}{2}; \frac{1}{2} \right)$$

498 Where $I_s(a, b)$ is the regularized β -function (the cumulative distribution of the β -distribution).
 499 In fact those two expression converge at high diversity S . In any case, we see here that the
 500 probability of underestimation will grow with S .

501 **S3 Effective diversity**

502 S may not always be the relevant measure of diversity. Indeed if $u_i = N_i^{\frac{p}{2}} u'_i$ where N_i is the
 503 abundance (or biomass) of species i and $C^{u'} \propto \mathbb{I}$ then $C^u \propto D^p$ where D is a diagonal matrix
 504 with $D_{ii} = N_i$. If v_i obeys a similar rule, so that $C^v \propto D^q$ then

$$\operatorname{Tr} C^u C^v \propto \|N\|_{\frac{p+q}{p+q}}^{p+q}$$

505 while

$$\operatorname{Tr} C^u \operatorname{Tr} C^v \propto \|N\|_p^p \|N\|_q^q$$

506 so that

$$\mathbb{E} \cos^2 \theta \simeq \frac{\|N\|_{\frac{p+q}{p+q}}^{p+q}}{\|N\|_q^q \|N\|_p^p} =: \frac{1}{\operatorname{IPR}_{q,p}(N)}$$

507 In particular, for $q = p = 2$ we get that

$$\mathbb{E} \cos^2 \theta \simeq \frac{1}{\operatorname{IPR}(N)}$$

508 where $\operatorname{IPR}(N)$ is the Inverse Participation Ratio, a measure of diversity of the abundance
 509 distribution N . The more general expression above can also be seen as a measure of effective

510 diversity. It can be compared to Hill's diversity metrics with index $Q = p + q$

$${}^Q D = \left(\sum p_i^Q \right)^{\frac{1}{1-Q}} = \left(\frac{\|N\|_1}{\|N\|_Q} \right)^{\frac{Q}{Q-1}} = \left(\frac{\|N\|_1^p \|N\|_1^q}{\|N\|_{p+q}^{p+q}} \right)^{\frac{1}{p+q-1}}$$

511 where p_i is the relative abundance of species i . We indeed see that ${}^Q D$ coincides with $\text{IPR}_{q,p}$
 512 when $q = p = 1$, and stays closely related in general. In fact, using the inequality

$$\|N\|_p \leq \|N\|_1 \leq S^{1-\frac{1}{p}} \|N\|_p; \quad p \geq 1$$

513 one gets, for $p, q \geq 1$

$$S^{2-Q} \times {}^Q D^{Q-1} \leq \text{IPR}_{q,p} \leq {}^Q D^{Q-1}$$

514 **S3.1 Probability of underestimation**

515 If $\cos \theta$ is approximately normally distributed with zero mean and variance $\sigma^2 = \frac{1}{S_{\text{eff}}}$ (where
 516 $S_{\text{eff}} \leq S$ would be an effective dimensionality as defined in the previous sections), then

$$\mathbb{P}(y \geq 0 : x) \simeq \frac{1}{2} \left[1 + \text{erf} \left(\frac{x}{2} \sqrt{\frac{S_{\text{eff}}}{2}} \right) \right]$$

517 This expression should be compared to the exact solution derived above in the case of a
 518 uniform sampling over the direction of u (the case if $u_i \sim \mathcal{N}(0, 1)$), which suggest the Ansatz

$$\mathbb{P}(y \geq 0 : x) = 1 - \frac{1}{2} I_{1-\frac{x^2}{2}} \left(\frac{S_{\text{eff}} - 1}{2}; \frac{1}{2} \right)$$

519 when the effective dimensionality is not necessarily S or even an integer (the two expressions
 520 uniformly converge towards one another as S_{eff} grows).

521 **S3.2 Projection on linear functions**

522 Suppose now that we measure S_F linear functions of species biomass of the form

$$F_\alpha(B) = \sum_{i=1}^S F_{\alpha,i} B_i \quad \alpha = 1, \dots, S_F$$

523 We must now project the covariance matrices onto the space spanned by the gradient ($F_{\alpha,i}$) of
 524 the functions. If $P_\alpha = (F_{\alpha,i}F_{\alpha,j})$ the projector on the function F_α , we can do this as

$$\mathbb{E}_{u,v} \cos^2 \theta_F \simeq \frac{\sum_{\alpha,\beta} \text{Tr} P_\alpha C^u P_\beta C^v}{\sum_{\alpha,\beta} \text{Tr} P_\alpha C^u \text{Tr} P_\beta C^v}$$

525 When taking an ensemble average of functions, with $\mathbb{E}P_\alpha = \mathcal{P} = (\mathbb{E}F_i F_j)$, we must take care
 526 in differentiating terms in sums for which $\alpha \neq \beta$ and terms where $\alpha = \beta$. In the former case
 527 the projectors P_α and P_β are independent random variables and we can replace them by their
 528 mean \mathcal{P} . In the latter case, we must first define \hat{P}_α as the linear operator that maps a matrix
 529 M to $P_\alpha M P_\alpha$; its ensemble mean $\hat{\mathcal{P}}$ encodes the 4th moments of F_α . We then get

$$\mathbb{E} \cos^2 \theta_F \simeq \frac{(S_F - 1) \text{Tr} \mathcal{P} C^u \mathcal{P} C^v + \text{Tr} \hat{\mathcal{P}}(C^u) C^v}{S_F \text{Tr} \mathcal{P} C^u \text{Tr} \mathcal{P} C^v}$$

530 **Example 1**

531 This example is the one treated in the main text, where the functions are statistically
 532 independent of one another. Suppose as before that $C^u = C^v = D^2$ ($p = q = 1$) and
 533 $\mathbb{E}F_i = 0$ $\mathbb{E}F_i F_j = \delta_{ij}$ (this condition is what we mean by statistically independent). One gets
 534 that

$$\mathbb{E} \cos^2 \theta_F \simeq \frac{1}{\text{IPR}} + \frac{1}{S_F} - \frac{1}{S_F} \frac{1}{\text{IPR}} = \frac{1}{S_{\text{eff}}}$$

535 so that at first order, the effective dimensionality S_{eff} is the harmonic mean

$$S_{\text{eff}} \approx \frac{1}{\frac{1}{S_F} + \frac{1}{\text{IPR}}}$$

536 as presented in Eq. (8)

537 **Example 2**

538 For the sake of completeness we treat here the case where the functions are not statistically
 539 independent due to the fact that $m_1 = \mathbb{E}(F_j) \neq 0$ (the average species contributions to functions
 540 tends to be either systematically positive or negative). In this case $\mathcal{P} = m_1^2 P_1 + (m_2 - m_1^2) \mathbb{I}$,
 541 where P_1 is a matrix whose elements are all equal to 1, and m_n are the n -th moments of F_i .
 542 We have that

$$\begin{aligned} \text{Tr}(\mathcal{P} D^2) &= \text{Tr}(m_1^2 P_1 D^2 + (m_2 - m_1^2) D^2) \\ &= m_2 \|N\|_2^2 \end{aligned}$$

543 and so

$$\text{Tr}(\mathcal{P}D^2)^2 = m_1^4 \|N\|_2^4 + (m_2^2 - m_1^4) \|N\|_4^4$$

544 on the other hand, one can show that

$$\text{Tr}\hat{\mathcal{P}}(D^2)D^2 = m_2^2 \|N\|_2^4 + (m_4 - m_2^2) \|N\|_4^4$$

545 if

$$\frac{1}{S_m} = \frac{m_1^4}{m_2^2}$$

546 we get that

$$\frac{(S_F - 1)\text{Tr}(\mathcal{P}D^2)^2}{S_F(\text{Tr}\mathcal{P}D^2)^2} = \frac{1}{S_m} + \frac{1}{\text{IPR}} - \frac{1}{S_m} \frac{1}{\text{IPR}} - \frac{1}{S_F} \frac{1}{S_m} - \frac{1}{S_F} \frac{1}{\text{IPR}} + \frac{1}{S_F} \frac{1}{S_m} \frac{1}{\text{IPR}}$$

547 on the other hand

$$\frac{1}{S_F} \frac{\text{Tr}\hat{\mathcal{P}}(D^2)D^2}{(\text{Tr}\mathcal{P}D^2)^2} = \frac{1}{S_F} - \frac{1}{S_F} \frac{1}{\text{IPR}} + \frac{m_4}{m_2^2} \frac{1}{S_F} \frac{1}{\text{IPR}}$$

548 summing the two gives

$$-\frac{1}{S_m} \frac{1}{\text{IPR}} - \frac{1}{S_F} \frac{1}{S_m} + \left(\frac{m_4}{m_2^2} - 2\right) \frac{1}{S_F} \frac{1}{\text{IPR}} + \frac{1}{S_F} \frac{1}{S_m} \frac{1}{\text{IPR}}$$

549

$$\begin{aligned} \mathbb{E} \cos^2 \theta_F \approx & \frac{1}{S_F} + \frac{1}{S_m} + \frac{1}{\text{IPR}} \\ & - \frac{1}{S_m} \frac{1}{\text{IPR}} - \frac{1}{S_F} \frac{1}{S_m} + \left(\frac{m_4}{m_2^2} - 2\right) \frac{1}{S_F} \frac{1}{\text{IPR}} \\ & + \frac{1}{S_m} \frac{1}{S_F} \frac{1}{\text{IPR}} \end{aligned}$$

550 for a normal distribution

$$m_4 = -2m_1^4 + 3m_2^2$$

551 thus

$$\frac{m_4}{m_2^2} - 2 = 1 - \frac{2}{S_m}$$

552 we then have

$$\begin{aligned} \mathbb{E} \cos^2 \theta_F \approx & \frac{1}{S_F} + \frac{1}{S_m} + \frac{1}{\text{IPR}} \\ & - \frac{1}{S_F} \frac{1}{S_m} - \frac{1}{S_F} \frac{1}{\text{IPR}} - \frac{1}{S_m} \frac{1}{\text{IPR}} - \frac{1}{S_m} \frac{1}{S_F} \frac{1}{\text{IPR}} \end{aligned}$$

553 We see here interactions between the various dimensions S_m , S_F and IPR, with a potential
 554 dominance of S_m when all other are much larger. This effective dimensionality emerges due to
 555 the collinearity of functions, which thus span a subspace of potentially much smaller dimension
 556 than S_F .

557 S3.3 Change of metric

558 Consider a non euclidean metric tensor H (i.e a positive definite matrix). Distances must now
559 be measured as

$$\|w\|^2 \rightarrow \langle w|Hw \rangle; \|v\|^2 \rightarrow \langle v|Hv \rangle; \|u\|^2 \rightarrow \langle u|Hu \rangle$$

$$y = \frac{\langle w|Hw \rangle - \langle v|Hv \rangle}{\langle v|Hv \rangle} = \frac{\langle u|Hu \rangle}{\langle v|Hv \rangle} + 2\sqrt{\frac{\langle u|Hu \rangle}{\langle v|Hv \rangle}} \frac{\langle u|Hv \rangle}{\sqrt{\langle v|Hv \rangle \langle u|Hu \rangle}}$$

$$y(x_H) = x_H^2 + 2x_H \frac{\langle u|Hv \rangle}{\sqrt{\langle v|Hv \rangle \langle u|Hu \rangle}}$$

$$\begin{aligned} \mathbb{E}_{u,v} \langle u|Hv \rangle^2 &= \mathbb{E}_{u,v} \langle v|Hu \rangle \langle uH|v \rangle \\ &= \mathbb{E}_v \langle v|HC^u H v \rangle \\ &= \text{Tr} C^v H C^u H \end{aligned}$$

$$\begin{aligned} \mathbb{E}_u \langle u|Hu \rangle &= \mathbb{E}_u \langle u|Hu \rangle \\ &= \text{Tr} C^u H \end{aligned}$$

560 Thus

$$\mathbb{E}_{u,v} \left(\frac{\langle u|Hv \rangle}{\sqrt{\langle v|Hv \rangle \langle u|Hu \rangle}} \right)^2 \approx \frac{\text{Tr} C^v H C^u H}{\text{Tr} C^v H \text{Tr} C^u H} = \frac{1}{S_H}$$

561 the change of metric can thus change the effective dimensionality. In particular, if $C^u \propto C^v \propto \mathbb{I}$
562 this gives

$$\frac{1}{S_H} = \frac{\sum_{i=1}^S \lambda_i^2}{(\sum_{i=1}^S \lambda_i)^2}$$

563 where λ_i are the eigenvalues of H . Note that H could be the Hessian function (second
564 derivatives) of a non linear function, computed near the initial state. This explains how
565 non linear functions can induce a dimensionality effect on the probability of underestimating
566 change, as illustrated in Fig. S1.

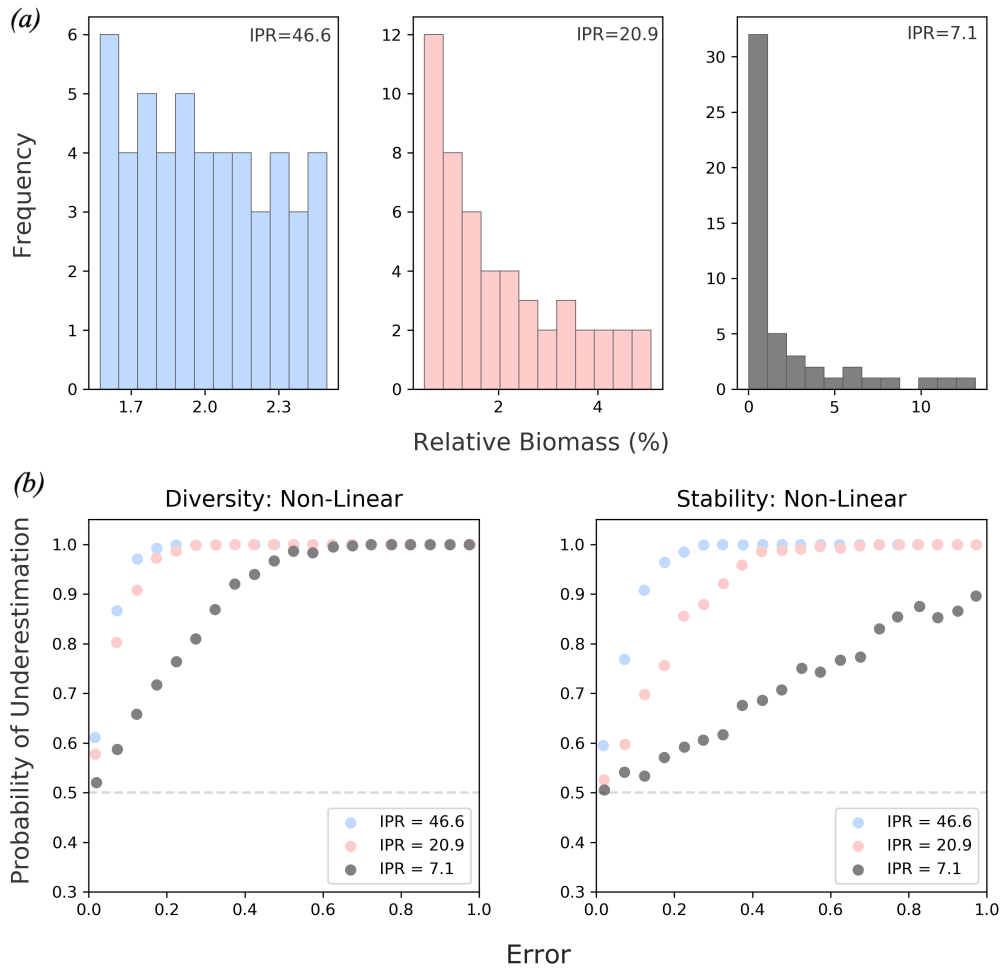


Figure S1: (a) Biomass distributions of three 50-species communities with IPR and therefore effective dimensionality of 46.6 (blue), 20.9 (red) and 7.1 (grey). (a) The non-linear contribution of diversity (the Shannon index) and stability (invariability) towards the probability of underestimation; it is the non-linear part of a function that is sensitive to the dimensionality of the underlying system.

567 S4 Simulations

568 Initially, the theoretical relationship between error, underestimation and dimensionality was
 569 tested using numerical simulations (Fig. 2(c)). These simulations uniformly sampled the
 570 intersecting circles, spheres and hyper-spheres defined by a prediction of change and relative
 571 error (Fig. 2). This was done for 1-D, 2-D, 10-D and 20-D systems over 20,000 simulations.
 572 Specifically:

- 573 • a prediction of change and was randomly generated from a normal distribution of mean
 574 0 and standard deviation 1 (defining the blue circle in Fig. 2a).

- 575 • a direction of error was randomly generated from a normal distribution of mean 0 and
576 standard deviation 1, and a magnitude of error was randomly generated from a uniform
577 distribution between 0 and 2 (defining the the red circle in Fig. 2a).
- 578 • From these values, error (x) and underestimation (y) were calculated based on Euclidean
579 distance and subsequently plotted in Fig. 2c).
- 580 • The probability of underestimation $P(y > 0; x)$ was calculated from the simulated results
581 of error and underestimation.

582 As a next step, these simulations were modified to fit ecological problems. In Fig. 1 and Fig. 4
583 the intersecting shapes that are uniformly sampled had dimensions determined by the number
584 of species in a simulated community. However, the dimensions of state space were given
585 unequal weighting of how they respond to change in the form of uneven biomass distributions
586 randomly generated from a log normal distribution of mean 0 and standard deviation 0.05.

587 In Fig. 3 and Fig. S1 communities of 50 species were given unequal biomass distributions by
588 drawing species' biomass from a log scale of varying range; the wider the range of the log
589 scale the more uneven the biomass distribution. Underestimation (y) was calculated using
590 Euclidean distance *and* a number of ecological relevant aggregate properties: the Shannon
591 index (diversity), invariability (stability) and total biomass (functioning).

592 For Fig. 5 our simulations were modified to illustrate that additional dimensional effects
593 come into play when changes in multiple functions are considered at once. Over 50,000
594 simulations 20-D hyper-spheres (community of 20 species) with unequal weighting (IPR of
595 9.9) were uniformly sampled and the results were projected into functional space. Specifically,
596 underestimation was measured for 1, 2, 3, 5 and 10 aggregate functions. Linear aggregate
597 functions of the form

$$F(B) = \sum_{i=1}^S F_i B_i$$

598 were defined via the coefficients F_i , i.e. their sensitivity to the change in the biomass of species
599 i . The sensitivity of an aggregate function to each species was randomly drawn from a normal
600 distribution of mean 0 and standard deviation 1. This corresponds to the case of statistically
601 independent functions (see example 1 in subsection S3.2). State space was then defined by the
602 number of functions.

603 Simulations were conducted in Python with the Matplotlib, NumPy and SciPy libraries.
604 Code is available in a Jupyter Notebook on GitHub: [https://github.com/jamesaorr/
605 scaling-up-uncertain-predictions](https://github.com/jamesaorr/scaling-up-uncertain-predictions).